

# Is there a common pattern of future gas-phase air pollution in Europe under diverse climate change scenarios?

Pedro Jiménez-Guerrero · Juan J. Gómez-Navarro ·  
Rocío Baró · Raquel Lorente · Nuno Ratola ·  
Juan P. Montávez

Received: 14 June 2012 / Accepted: 18 September 2013 / Published online: 15 October 2013  
© Springer Science+Business Media Dordrecht 2013

**Abstract** Climate change alone influences future levels of tropospheric ozone and their precursors through modifications of gas-phase chemistry, transport, removal, and natural emissions. The goal of this study is to determine at what extent the modes of variability of gas-phase pollutants respond to different climate change scenarios over Europe. The methodology includes the use of the regional modeling system MM5 (regional climate model version)-CHIMERE for a target domain covering Europe. Two full-transient simulations covering from 1991–2050 under the SRES A2 and B2 scenarios driven by ECHO-G global circulation model have been compared. The results indicate that the spatial patterns of variability for tropospheric ozone are similar for both scenarios, but the magnitude of the change signal significantly differs for A2 and B2. The 1991–2050 simulations share common characteristics for their chemical behavior. As observed from the NO<sub>2</sub> and  $\alpha$ -pinene modes of variability, our simulations suggest that the enhanced ozone chemical activity is driven by a number of parameters, such as the warming-induced increase in biogenic emissions and, to a lesser extent, by the variation in nitrogen dioxide levels. For gas-phase pollutants, the general increasing trend for ozone found under A2 and B2 forcing is due to a multiplicity of climate factors, such as increased temperature, decreased wet removal associated with an overall decrease of precipitation in southern Europe, increased

---

**Electronic supplementary material** The online version of this article (doi:10.1007/s10584-013-0944-8) contains supplementary material, which is available to authorized users.

P. Jiménez-Guerrero (✉) · J. J. Gómez-Navarro · R. Baró · R. Lorente ·  
N. Ratola · J. P. Montávez

Regional Campus of International Excellence “Campus Mare Nostrum”,  
University of Murcia, Campus de Espinardo, 30100 Murcia, Spain  
e-mail: pedro.jimenezguerrero@um.es

J. J. Gómez-Navarro  
Climate and Environmental Physics and Oeschger Centre for Climate Change Research,  
University of Bern, Bern, Switzerland

photolysis of primary and secondary pollutants as a consequence of lower cloudiness and increased biogenic emissions fueled by higher temperatures.

## 1 Introduction

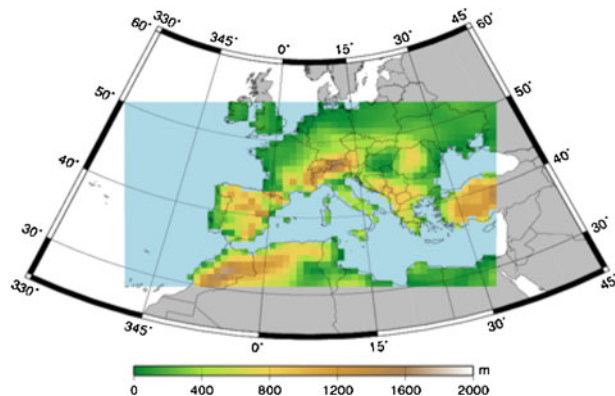
The impact of climate change on air pollution, especially on gas-phase pollutants and ozone, has been previously described in a number of studies (e.g. Forkel and Knoche 2006; Szopa et al. 2006; Giorgi and Meleux 2007; Meleux et al. 2007; Kruger et al. 2008; Katragkou et al. 2010; Anderson and Engardt 2010; Katragkou et al. 2011, among many others). Variations in climate affect gas-phase pollutants by changing the dispersion (wind speed, mixing layer height, convective fronts), deposition by precipitation, dry deposition, photochemistry, natural emissions and background concentrations (Zlatev and Moseholm 2008; Jacob and Winner 2009). Hence, the effects of climate change on air quality should be studied in the broader context of chemistry-climate interactions (Giorgi and Meleux 2007; Gustafson and Leung 2007). Most of the aforementioned works use the future-minus-present method to assess the future impacts on air quality, selecting present and future time-slices of simulations. However, we should bear in mind that this approach is sensitive to the chosen control and future periods due to the inherent internal variability of the climate models, especially at regional scales (Raisanen et al. 2004; Gómez-Navarro et al. 2011). In this sense, the Empirical Orthogonal Functions (EOFs) methodology (Zorita et al. 2005; Monahan et al. 2009) is able to reduce the uncertainty associated to the internal variability when applied to full transient simulations due to the longer time series obtained. However, this methodology is not widely used in air quality-climate change studies due to the computational cost involved.

The magnitude and extent of potential impacts of climate change on air quality in Europe urged major government agencies to undertake several important actions in this regard. The impact studies to be performed under this umbrella inevitably require downscaled scenarios of air quality under climate change scenarios, with as high spatial resolution as possible. The wide spread in the results of recent studies trying to analyze the influence of climate change on regional air pollution pointed out by Racherla and Adams (2008) and Wu et al. (2008), among others, indicate their inherent difficulty.

Avise et al. (2009) highlighted the need for further works (especially in other regions apart from the United States) in order to assess the potential impact of global changes on regional air quality. In this sense, air quality projections at a regional scale are affected by several sources of uncertainty, being the election of the emission scenario one of the most important contributors to the spread of the results. Therefore, a problem arising is to check whether the projected air quality is dependent, and to what extent, on the SRES scenario selected. In this sense, Gómez-Navarro et al. (2010) found that the spatial structure of the warming patterns depends neither on the emission scenario nor on the global circulation model used to drive the regional simulations. It is, rather, an inherent feature of the target domains covered by the regional model.

As such, the aim of this work is to check whether the projected changes in gas-phase air pollution over Europe depends on the scenario driving the regional simulation. For this purpose, two full-transient regional climate change-air quality projections for the first half of the XXI century (1991–2050) has been carried out, including A2 and B2 SRES scenarios.

**Fig. 1** Topography (m) of the domain included in the study as incorporated in the MM5-RCM model



## 2 Models and methods

The regional modeling system consists on MM5 regional climate model and CHIMERE chemistry transport model (coupled off-line) according to the work of Jiménez-Guerrero et al. (2011, 2012). The spatial model configuration comprises a domain of MM5-RCM simulations covering most of Europe with a resolution of 25 km (Fig. 1). Twenty-four sigma levels are considered in the vertical, with the top at 100 hPa. The fields are interpolated to CHIMERE working grids (resolution of about 0.25° for the European domain, in that order).

The climate and air quality simulations cover two full-transient simulations, from 1991 to 2050, driven by ECHO-G General Circulation Model under the SRES A2 and B2 scenarios. In order to isolate the possible effects of climate change on the ground concentrations of gas-phase air pollution, unchanged anthropogenic emissions (derived from EMEP database) are assumed. Natural emissions depend on climate conditions, and are the only ones to vary between reference and future climate simulations. Therefore, the effects of climate change on air pollutants are estimated excluding possible changes on vegetation, land use, anthropogenic pollutant emission changes or any feedbacks from the chemical compounds to the climatological fields, yet allowing changes in natural biogenic emissions (Meleux et al. 2007).

For a more detailed description on the physicochemical parameterizations and the performance of the model to reproduce present-day air quality climatologies, the reader is referred to the [Supplementary Material](#).

### 2.1 Empirical Orthogonal Functions (EOFs)

In order to investigate the concentration signal along the first half of the XXI century, we apply a principal component analysis that decomposes the air pollution and climatological fields into Empirical Orthogonal Functions (EOFs) characterizing space patterns of variability and their associated Principal Components (PCs), representing their temporal evolution. This methodology allows the increase of the signal-to-noise ratio with respect to the original series, reducing the high dimensionality of complex phenomena and summarizing its main properties in a much smaller number of prominent variability modes (Hannachi et al. 2007). The EOFs analysis is

conducted on the geophysical fields. Here, annual series of modeled air pollution for O<sub>3</sub> maximum concentrations, mean NO<sub>2</sub>,  $\alpha$ -pinene (as a surrogate representing the BVOCs concentration) and climatological values (corresponding to the first layer of the model, approx. 15 m, for the period 1991–2050) are used. Following Fiore et al. (2003) we construct a covariance matrix of elements  $r_{ij}$  representing the correlation of anomalies between grid square i and grid square j over the first half of the XXI century. The EOFs are the eigenvectors of the correlation matrix and represent linear independent modes of variability. The sum of all eigenvalues equals the total variance in the original data.

The first EOF (EOF1) is selected from the eigenvectors as that accounting for the largest percentage of variance explained of the original dataset. When much of the original variance can be represented only with the EOF1, this methodology is a useful data reduction technique applied to air quality data and modeling results. The projection of the pollutants concentration or climatological fields onto the EOFs defined the principal components; these time series describe the temporal variation in the contribution of the associated EOF to the total variance. In our case, for the analysis we will focus on EOF1 and the associated PC1, since EOF1 captures the global trend and EOFs beyond the first individually account for less than 5 % of the total variance.

We further analyze the spatial correlations of EOF1 between air pollutants in the two scenarios, A2 and B2, which is an index of the similarity between the spatial patterns of variation, and also the temporal correlation of PC1s, depicting the temporal evolution associated to the spatial pattern of change. We also applied a Mann-Kendall test to the PC1 of these variables in order to obtain the statistical significance of the obtained trends. This non-parametric test is widely used in climate studies and is capable to detect the trends or inhomogeneities in the series of data.

### 3 Results

#### 3.1 Spatio-temporal patterns of variability

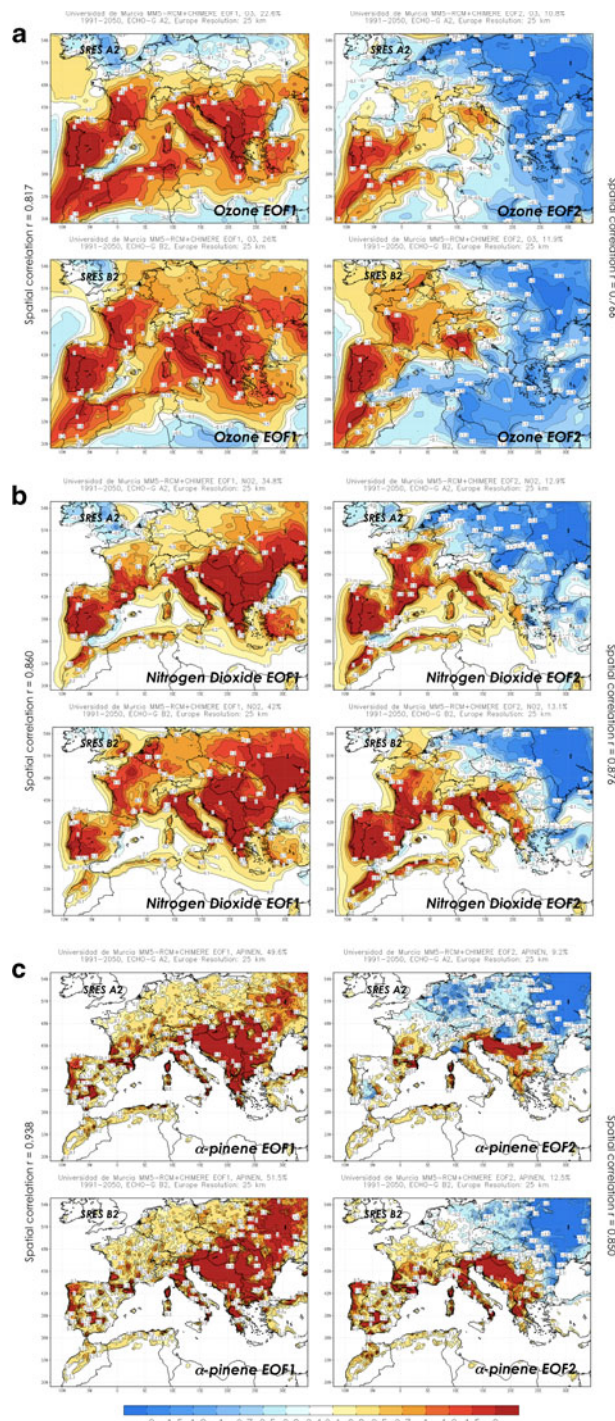
The EOFs and PCs are extracted from our modeling results for the 1991–2050 period both for the concentrations of gas-phase pollutants and for those climatological variables (in both scenarios) whose change would have a significant impact on pollution levels (Wu et al. 2008).

In order to check whether the air quality patterns are dependent on the SRES scenario selected, the spatial correlations between EOF1 in the A2 and B2 experiments for O<sub>3</sub>, NO<sub>2</sub> and  $\alpha$ -pinene have been calculated. The analysis of the PCs beyond the first present no significant trend ( $p > 0.1$ ), according to the Mann-Kendall test performed, and hence it is EOF1 which conditions the variation pattern and the rest of the section will focus on EOF1, as advised by Jiménez-Guerrero et al. (2011).

The EOF1 accounts for around 23 % (25 %) of the total variance for O<sub>3</sub> levels, 35 % (42 %) for NO<sub>2</sub> and 50 % (51 %) for  $\alpha$ -pinene under the A2 (B2) scenario. Figure 2 represents the spatial correlation found between A2 and B2 scenarios for EOF1 and EOF2, just to indicate that, despite it is EOF1 which supports the trend, there is also a strong correlation for the second empirical orthogonal function.

For O<sub>3</sub>, the high spatial correlations found between A2 and B2 scenarios ( $r = 0.817$  for EOF1 and  $r = 0.766$  for EOF2) suggest that the spatial patterns of future

**Fig. 2** **a** EOF1 (left) and EOF2 (right) for O<sub>3</sub> under the SRES A2 (top) and B2 (bottom) scenarios. The correlation coefficients for both EOFs are depicted in the figure. **b** Id. for NO<sub>2</sub>. **c** Id. for  $\alpha$ -pinene



variation of O<sub>3</sub> pollution over Europe (Fig. 2) hardly change with a different scenario. As observed from NO<sub>2</sub> and  $\alpha$ -pinene patterns (Fig. 2, bottom) under the A2 and B2 scenario, the modes of variability for those pollutants and scenarios are even more correlated than those for O<sub>3</sub> ( $r = 0.869$  and  $r = 0.876$  for EOF1 and EOF2, in the case of NO<sub>2</sub>, and  $r = 0.938$  and  $r = 0.850$  for the biogenic species).

One important result is that the modes of variability of O<sub>3</sub> are highly correlated with those of NO<sub>2</sub> and  $\alpha$ -pinene. If establishing the spatial correlation between O<sub>3</sub> and their precursors, O<sub>3</sub>-correlation coefficients are  $r = 0.640(0.691)$  with NO<sub>2</sub> and  $r = 0.803(0.746)$  with  $\alpha$ -pinene in the A2(B2) scenario. In this sense, Jiménez-Guerrero et al. (2011) identified the warming-induced increase in biogenic emissions as the main cause of variation of future O<sub>3</sub> concentrations, especially in southwestern Europe.

The increasing trends, as derived from the PC1, are significant ( $p < 0.01$ ) for the first principal component of O<sub>3</sub>, NO<sub>2</sub> and  $\alpha$ -pinene in both scenarios. There is a positive trend in the O<sub>3</sub> series found under A2 and B2 forcing (which only differ in the slope of the trend, and thus, in the intensity of the signal). This involves an increase of future O<sub>3</sub> concentrations in all Europe (except in the northernmost areas of Europe under the A2 scenario, where the concentrations, as shown by EOF1, will remain invariant or even slightly decrease) (Fig. 2). Albeit results for A2 and B2 are analogous, B2 trends are slightly lower than those for A2 scenario (Fig. 3).

The co-increase in the trend for O<sub>3</sub> precursors in both scenarios is noticeable, as the O<sub>3</sub> formation is dependent on the NO<sub>x</sub>/VOC ratio (Jiménez and Baldasano 2004). Moreover, Meleux et al. (2007) indicate that a higher future biogenic reactivity sustains the O<sub>3</sub> production cycle and increases the O<sub>3</sub> yield per NO<sub>x</sub> molecule.

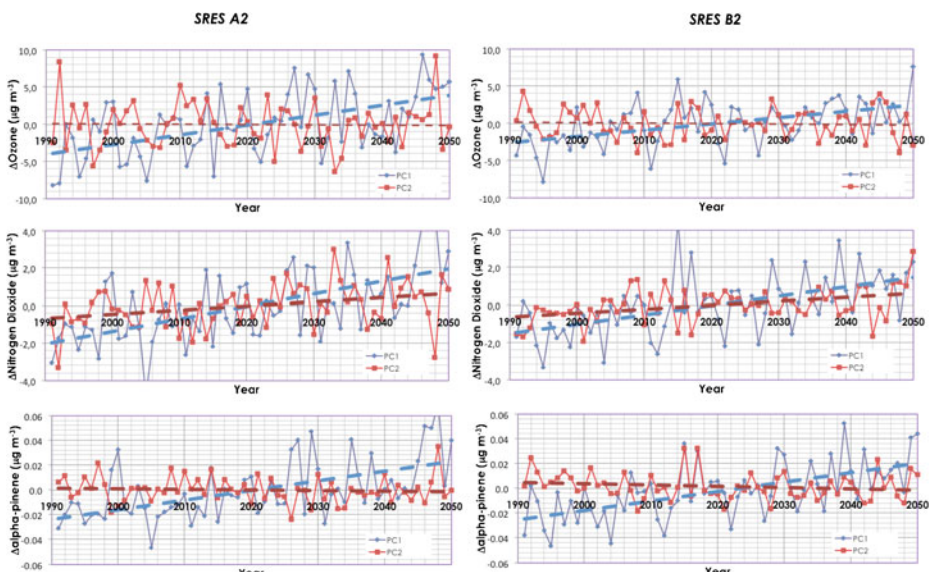


**Fig. 3** First (PC1) and second (PC2) principal component for O<sub>3</sub>, NO<sub>2</sub> and  $\alpha$ -pinene

### 3.2 Correlation with climatological parameters

The shapes of the spatial patterns for air pollutants seem to be related with several patterns of future change for climatological parameters. Here we focus on temperature, precipitation, mixing height and cloudiness (cloud cover) as the most important climatological variables conditioning the gas-phase concentrations of pollutants. Table 1 represents the spatial correlation between these variables and O<sub>3</sub> and its precursors in the A2 and B2 scenarios, while Fig. 4 shows the respective EOF1. In this case, only the EOF1 for the A2 scenario has been included, since the spatial patterns for A2 and B2 scenario present a similar structure (spatial correlation of 0.989 for temperature, 0.917 for total precipitation, 0.904 for mixing height and 0.820 for cloudiness). As stated for gas-phase pollutants, the EOF1 alone explains most of the variability for these climatological variables (around 90 % for temperature and precipitation and around 40 % for mixing height and cloudiness) and thus our analysis focuses just on this first empirical orthogonal function.

The EOF1 for temperature can be associated to the spatial structure of the future warming pattern, more intensified towards southern Europe (Gómez-Navarro et al. 2010). However, this spatial pattern is not strongly correlated to O<sub>3</sub> on either the A2 ( $r = 0.425$ ) and the B2 scenario ( $r = 0.557$ ). So, future O<sub>3</sub> patterns do not seem to be directly related to those of temperature (although O<sub>3</sub> increases are influenced by the temperature variations). The only patterns of variability that seem to be related, and hence present a similar shape, are those for temperature and  $\alpha$ -pinene ( $r = 0.702$  and  $r = 0.658$  for the A2 and B2 scenarios, in that order), since the spatial correlation with NO<sub>2</sub> is notably lower ( $r = 0.217(0.475)$  for the A2(B2) scenario).

Moreover, the variations (general decreases in southern Europe) in precipitation for the future scenario can strongly influence the levels of NO<sub>2</sub> (the variation patterns of this pollutant and precipitation are somehow related, with  $r = -0.563(-0.568)$  for A2(B2) scenarios), since the wet deposition of nitric acid (HNO<sub>3</sub>) is the main sink for NO<sub>x</sub>. In the existence of sunlight, NO<sub>2</sub> reacts mainly with hydroxyl radical to produce HNO<sub>3</sub>, while nighttime chemistry involves the formation of N<sub>2</sub>O<sub>5</sub>, the anhydride of HNO<sub>3</sub>, whose dry and wet deposition can be an important nighttime loss process for nitrogen oxides (Atkinson 2000; Jacob 2000).

The changes in ventilation and, specifically, in the mixing height have strong effects on the concentrations of gas-phase pollutants. The mixing height (MH) modes of variability over land show an important north-south behavior, with a decreasing trend over land in southern Europe and increases over higher latitudes (Fig. 4). However, modifications in the MH are generally less than 20 %. As expected, a strong correlation of air pollutants with stagnant conditions is found, as previously reported by Leung and Gustafson (2005). The modes of variability for MH show

**Table 1** Spatial correlation coefficients between the modes of variability of climatological variables and gas-phase pollutants in the A2(B2) scenarios over land

Variable	O <sub>3</sub>	NO <sub>2</sub>	$\alpha$ -pinene
Temperature	0.425 (0.557)	0.217 (0.475)	0.702 (0.658)
Precipitation	-0.364 (-0.299)	-0.563(-0.568)	-0.167 (-0.212)
Mixing height	-0.686 (-0.685)	-0.602(-0.588)	-0.658 (-0.686)
Cloudiness	0.708 (0.653)	0.442(0.417)	0.210 (0.251)

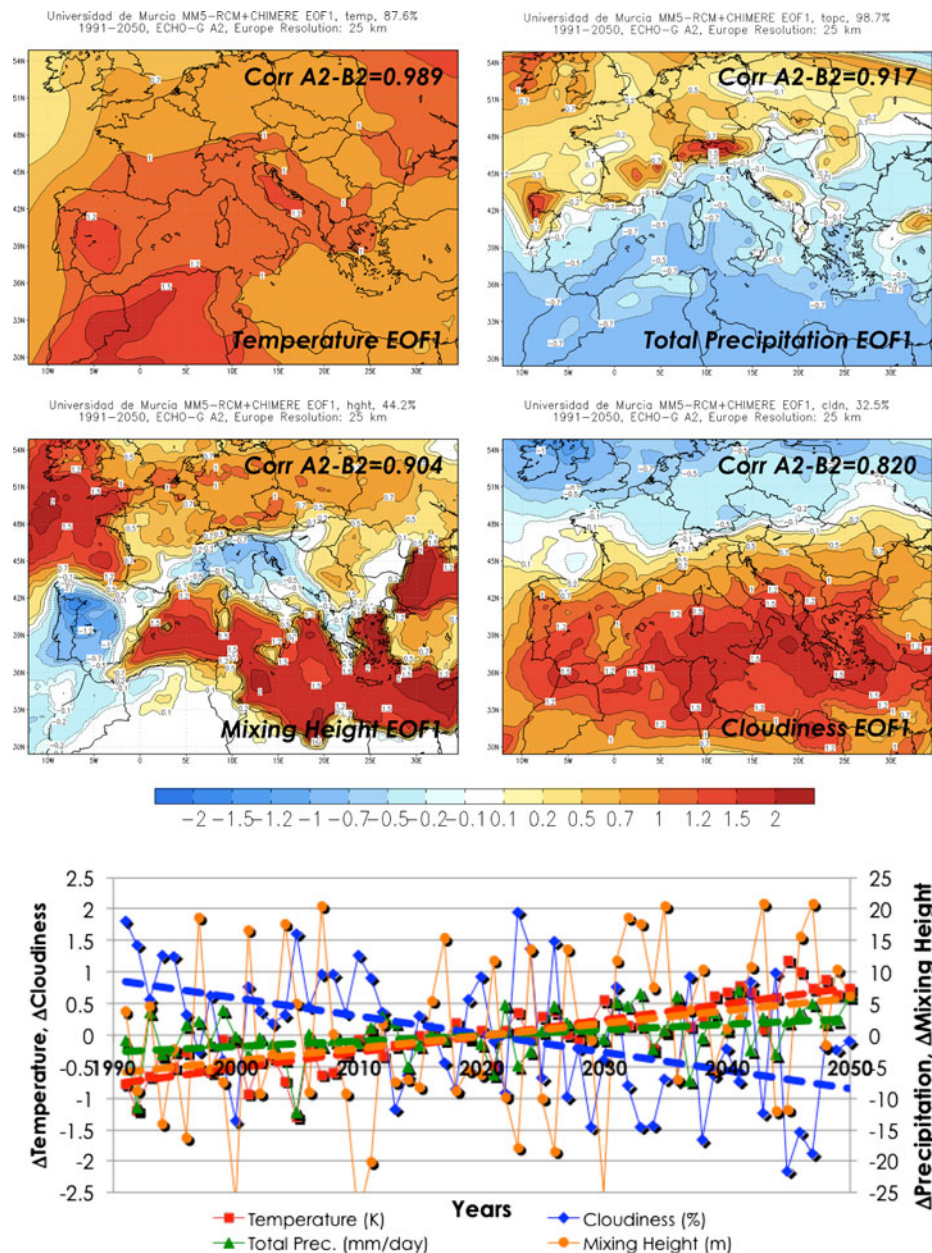


**Fig. 4** (Top) EOF1 for temperature, total precipitation, mixing height and cloudiness. The number in the figure represents the spatial correlation between the EOF1 of A2 and B2 scenario. (Bottom) PC1 of the corresponding climatological variables

a strong anticorrelation with those of  $O_3$  ( $r = -0.686$  for A2 and  $r = -0.685$  for B2 scenarios),  $NO_2$  ( $r = -0.602$  and  $r = -0.588$  for A2 and B2 scenarios, in that order) and  $\alpha$ -pinene, with  $r = -0.658(-0.686)$  for the A2(B2) scenario. Note that

the decreases in the MH over land (hampering dispersion processes) are generally associated with a pattern indicating decreasing precipitation and important increases of temperatures (e.g. Iberian Peninsula), therefore representing an adding effect. Thus, the future O<sub>3</sub> increase may be caused by the future combination of less dispersive conditions and lower removal efficiency simulated analogously in both scenarios, leading to increased concentrations of pollutants in the boundary layer, and particularly by an enhancement of NO<sub>2</sub> availability over most of Europe.

Finally, the spatial pattern for cloudiness (cloud fraction) shows a strong north-south dipole. In our case, the maximum decrease occurs over southern Europe, as reported by Giorgi et al. (2004), while the strongest increases are observed over the northern areas, such as the British Isles or northern Germany. In this sense, our results agree with those by Katragkou et al. (2011), who identify a prominent decrease of cloudiness mostly over western Europe at the end of the XXI century associated with an anticyclonic anomaly which favors more stagnant conditions (and weakening of the westerly winds for southern Europe). This change in cloudiness is known to affect strongly the incoming solar radiation, and consequently the spatial patterns of O<sub>3</sub> by modifying its photochemical cycle. The spatial pattern of tropospheric O<sub>3</sub> is correlated ( $r > 0.65$  in both scenarios) to the mode of variability for cloudiness (but the PC1s are therefore anti-correlated) and show no important similarity in the spatial pattern for the rest of precursors ( $r < 0.45$ ).

#### 4 Conclusions

This work intended to highlight how future climate change can influence the modes of variability of gas-phase pollutants over Europe for the first half of the XXI century. For that, a regional climate modeling system (coupling MM5-RCM and CHIMERE chemistry transport model) has been applied to two full-transient simulations (1991–2050) driven by SRES A2 and B2 scenarios in order to obtain regional patterns of change for both climatological parameters and air pollutants. Results show the plausible influence of climate change alone on the levels of gas-phase pollutants.

Our simulations suggest that the modes of variability for tropospheric O<sub>3</sub> and their main precursors hardly change under different SRES scenarios, but the PC1 trends are higher for the A2 scenario with respect to the B2-driven simulation. Thus, the effect of changing scenarios has to be sought in the intensity of the changing signal, rather than in the spatial structure of the variation patterns, since the correlation between the spatial patterns of variability in A2 and B2 simulation is  $r > 0.75$  for all gas-phase pollutants included in this study. In both cases, full-transient simulations indicate an enhanced O<sub>3</sub> chemical activity under future scenarios.

The causes for tropospheric O<sub>3</sub> variations have to be sought in a multiplicity of climate factors, such as increased temperature, different distribution of precipitation patterns across Europe, increased photolysis of primary and secondary pollutants due to lower cloudiness, etc. Nonetheless, according to the results of this work future O<sub>3</sub> is conditioned by the dependence of biogenic emissions on the climatological patterns of variability. In this sense, O<sub>3</sub> over Europe is mainly driven by the warming-induced increase in biogenic emitting activity (vegetation is kept invariable in the simulations, but MEGAN estimations of these emissions strongly depends on shortwave radiation and temperature, which are substantially modified in climatic simulations). Moreover, one of the most important drivers for O<sub>3</sub> increase is the

decrease of cloudiness (related to stronger solar radiation) mostly over southern Europe at the first half of the XXI century. However, given the large uncertainty isoprene sensitivity to climate change (Guenther et al. 2006; Forkel and Knoche 2006; Horowitz et al. 2007) and the large uncertainties associated to the cloudiness projections, these results should be carefully considered.

As stated by Gómez-Navarro et al. (2010) the climatic response under different SRES scenarios is quite similar regarding the spatial structure of the leading variability modes for both temperature and precipitation. Hence, the leading mode of variability of gas-phase pollutants is expected to show a similar spatial structure in both scenarios, independently on which period the comparison focuses on (which is one of the strengths of the methodology presented on this work). The largest climatic differences among scenarios are however in the temporal component of this variability, being the larger trend under the A2 scenario the most apparent one.

However, the shape of these modes depends on the climatic modes, which at some extent also depend on the climatic model driving the simulations. Thus, some differences can be expected if the same results are obtained with different climate models. Moreover, it should be highlighted that the aforementioned results depend on the fact that the configuration of the modeling system (physical parameterizations, chemical mechanism, chemistry-driving conditions and domain) are equal in all simulations. Further simulations should be performed modifying these factors. Such sensitivity studies would be helpful in assessing the uncertainties linked to the dynamic downscaling process itself. Hence, future works should be devoted to investigate the differences in air pollution meteorology between diverse parameterizations in the chemistry transport models (physics, anthropogenic and natural emissions, chemistry, deposition), the impact of long-range transport in future air quality projections and the improvement from ensemble-based results of regional air quality-climate simulations.

**Acknowledgements** This work was funded by the Spanish Ministry of Economy and Competitiveness (CORWES CGL2010-22158-C02-02) and the European Regional Development Fund (FEDER). Dr. Pedro Jiménez-Guerrero acknowledges the Ramón y Cajal Programme. Dr. Nuno Ratola thanks the Marie Curie Action U-IMPACT from the University of Murcia. Simulations were carried out in the Ben Arabí Supercomputer of the Fundación Parque Científico de Murcia.

## References

- Andersson C, Engardt M (2010) European ozone in a future climate: important changes in dry deposition and isoprene emissions. *J Geophys Res* 115:D02303. doi:[10.1029/2008JD011690](https://doi.org/10.1029/2008JD011690)
- Atkinson R (2000) Atmospheric chemistry of VOCs and NOx. *Atmos Environ* 34:2063–2101
- Avise J, Chen J, Lamb B, Wiedinmyer C, Guenther A, Salathe E, Mass C (2009) Attribution of projected changes in summertime US O<sub>3</sub> and PM2.5 concentrations to global changes. *Atmos Chem Phys* 9:1111–1124
- Fiore AM, Jacob DJ, Mathur R, Martin RV (2003) Application of empirical orthogonal functions to evaluate O<sub>3</sub> simulations with regional and global models. *J Geophys Res* 108(D14):4431. doi:[10.1029/2002JD003151](https://doi.org/10.1029/2002JD003151)
- Forkel R, Knoche R (2006) Regional climate change and its impact on photo-oxidant concentrations in southern Germany: simulations with a coupled regional chemistry-climate model. *J Geophys Res* 111:D12302
- Giorgi F, Meleux F (2007) Modeling the regional effects of climate change on air quality. *Compt Rendus Geosci* 339:721–733
- Giorgi F, Bi X, Pal J (2004) Mean, interannual variability and trends in a regional climate change experiment over Europe. I: Climate change scenarios (2071–2100). *Clim Dyn* 23:839–858. doi:[10.1007/s00382-004-0467-0](https://doi.org/10.1007/s00382-004-0467-0)

- Gómez-Navarro JJ, Montávez JP, Jiménez-Guerrero P, Jerez S, García-Valero JA, González-Rouco JF (2010) Warming patterns in regional climate change projections over the Iberian Peninsula. *Meteorol Z* 19(3):275–285
- Gómez-Navarro JJ, Montávez JP, Jerez S, Jiménez-Guerrero P, Lorente-Plazas R, González-Rouco JF, Zorita E (2011) A regional climate simulation over the Iberian Peninsula for the last millennium. *Clim Past* 7:451–472. doi:[10.5194/cp-7-451-2011](https://doi.org/10.5194/cp-7-451-2011)
- Guenther A, Karl T, Harley P, Wiedinmyer C, Palmer PI, Geron C (2006) Estimates of global terrestrial isoprene emissions using MEGAN (Model of Emissions of Gases and Aerosols from Nature). *Atmos Chem Phys* 6:3181–3210
- Gustafson WI Jr, Leung LR (2007) Regional downscaling for air quality assessment. *Bull Am Met Soc* 88:1215–1227
- Hannachi A, Joliffe I, Stephenson W (2007) Empirical Orthogonal Functions and related techniques in atmospheric science: a review. *Int J Climatol* 27:1119–1152
- Horowitz LW, Fiore AM, Milly GP, Cohen RC, Perring A, Woolridge JP, Hess PG, Emmons LK, Lamarque J-F (2007) Observational constraints on the chemistry of isoprene nitrates over the eastern United States. *J Geophys Res* 112:D12508
- Jacob DJ (2000) Heterogeneous chemistry and tropospheric ozone. *Atmos Environ* 34:2131–2159
- Jacob DJ, Winner DA (2009) Effect of climate change on air quality. *Atmos Environ* 43:51–63
- Jiménez P, Baldasano JM (2004) Ozone response to precursor controls in very complex terrains: use of photochemical indicators to assess O<sub>3</sub>-NO<sub>x</sub>-VOC sensitivity in the northeastern Iberian Peninsula. *J Geophys Res* 109:D20309. doi:[10.1029/2004JD004985](https://doi.org/10.1029/2004JD004985)
- Jiménez-Guerrero P, Gómez-Navarro JJ, Jerez S, Lorente-Plazas R, García Valero JA, Montávez JP (2011) Isolating the effects of climate change in the variation of secondary inorganic aerosols (SIA) in Europe for the 21st century (1991–2100). *Atmos Environ* 45(4):1059–1063. doi:[10.1016/j.atmosenv.2010.11.022](https://doi.org/10.1016/j.atmosenv.2010.11.022)
- Jiménez-Guerrero P, Montávez JP, Gómez-Navarro JJ, Jerez S, Lorente-Plazas R (2012) Impacts of climate change on ground level gas-phase pollutants and aerosols in the Iberian Peninsula for the late XXI century. *Atmos Environ* 55:483–495. doi:[10.1016/j.atmosenv.2012.02.048](https://doi.org/10.1016/j.atmosenv.2012.02.048)
- Katragkou E, Zanis P, Tegoulias I, Melas D, Kruger BC, Huszar P, Halenka T, Rauscher S (2010) Decadal regional air quality simulations over Europe in present climate: near surface ozone sensitivity to external meteorological forcing. *Atmos Chem Phys* 10:11805–11821. doi:[10.5194/acp-10-11805-2010](https://doi.org/10.5194/acp-10-11805-2010)
- Katragkou E, Zanis P, Kioutsioukis I, Tegoulias I, Melas D, Kruger BC, Coppola E (2011) Future climate change impacts on summer surface ozone from regional climate-air quality simulations over Europe. *J Geophys Res* 116:D22307. doi:[10.1029/2011JD015899](https://doi.org/10.1029/2011JD015899)
- Kruger BC, Katragkou E, Tegoulias I, Zanis P, Melas D, Coppola E, Rauscher S, Huszar P, Halenka T (2008) Regional photochemical model calculations for Europe concerning ozone levels in a changing climate. *Q J Hungarian Meteorol Serv* 112(3–4):285–300
- Leung LR, Gustafson WI Jr (2005) Potential regional climate and implications to US air quality. *Geophys Res Lett* 32:L16711. doi:[10.1029/2005GL022911](https://doi.org/10.1029/2005GL022911)
- Meleux F, Solomon F, Giorgi F (2007) Increase in summer European O<sub>3</sub> amounts due to climate change. *Atmos Environ* 41:7577–7587. doi:[10.1016/j.atmosenv.2007.05.048](https://doi.org/10.1016/j.atmosenv.2007.05.048)
- Monahan AH, Fyfe JC, Ambaum MHP, Stephenson DB, North GR (2009) Empirical Orthogonal Functions: the medium is the message. *J Clim* 22:6501–6514
- Racherla PN, Adams PJ (2008) The response of surface O<sub>3</sub> to climate change over the Eastern United States. *Atmos Chem Phys* 8:871–885
- Raisanen J, Hansson U, Ullerstig A, Doscher R, Graham LP, Jones C, Meier HEM, Samuelsson P, Willen U (2004) European climate in the late twenty-first century: regional simulations with two driving global models and two forcing scenarios. *Clim Dyn* 22:13–31
- Szopa S, Hauglustaine DA, Vautard R, Menut L (2006) Future global tropospheric ozone changes and impact on European air quality. *Geophys Res Lett* 33:L14805. doi:[10.1029/2006GL025860](https://doi.org/10.1029/2006GL025860)
- Wu S, Mickley LJ, Leibensperger EM, Jacob DJ, Rind D, Streets DG (2008) Effects of 2000–2050 global change on O<sub>3</sub> air quality in the United States. *J Geophys Res* 113(D06302). doi:[10.1029/2007JD008917](https://doi.org/10.1029/2007JD008917)
- Zlatev Z, Moseholm L (2008) Impact of climate changes on pollution levels in Denmark. *Ecol Model* 217:205–219
- Zorita E, González-Rouco JF, von Storch H, Montávez JP, Valero F (2005) Natural and anthropogenic modes of surface temperature variations in the last thousand years. *Geophys Res Lett* 32:755–762